JCTC Journal of Chemical Theory and Computation

Toward Understanding the Photochemistry of Photoactive Yellow Protein: A CASPT2/CASSCF and Quantum Theory of Atoms in Molecules Combined Study of a Model Chromophore in Vacuo

P. B. Coto,*,† D. Roca-Sanjuán,† L. Serrano-Andrés,† A. Martín-Pendás,‡ S. Martí,§ and J. Andrés*,§

Instituto de Ciencia Molecular (ICMOL), Universidad de Valencia, Apdo. 22085, ES-46071, Valencia, Spain, Departamento de Química-Física y Analítica, Facultad de Química, Universidad de Oviedo, 33006, Oviedo, Spain, Departamento de Química-Física y Analítica, Universidad Jaume I, 224, 12071, Castellón, Spain

Received June 17, 2009

Abstract: Photochemical processes that take place in biological molecules have become an increasingly important research topic for both experimentalists and theoreticians. In this work, we report the reaction mechanism of a model of the photoactive yellow protein (PYP) chromophore in vacuo. The results obtained here, using a strategy based on the simultaneous use of the minimum energy path concept and the quantum theory of atoms in molecules applied to this excited state process, suggest a possible way in which the protein could increase the efficiency of the reaction. The role played by other electronic states of the same and different spin multiplicities in the reaction process is also analyzed, with special emphasis on that played by the lowest-lying triplet state. The possibility of a more complex than expected reaction mechanism is finally discussed, with some suggestions on the possible roles of the protein.

1. Introduction

The photoactive yellow protein (PYP) is a cytosolic protein found in certain types of bacteria. It works as a sensor, being responsible for the negative phototactic response of these bacteria when exposed to blue light.[1,2] The protein uses its chromophore, the *p*-hydroxycinnamoyl anion, as a molecular motor able to transform the energy of light into chemical work. This energy is employed for the modification of the conformation of the chromophore in the protein through a fast trans-to-cis isomerization process, part of which takes place in an excited electronic state. This change in the structure of the chromophore ultimately prompts a series of conformational changes in the protein structure that lead to the generation of a response of the organism, which moves away from the blue light source.

Together with rhodopsin, PYP is perhaps one of the most exhaustively studied protein photoreceptors, both experimentally[1,2] and theoretically.[3−13] The most accepted mechanism for the early events of the photocycle, based on experimental measurements[1,2,14] and molecular dynamics simulations,[6,7] points to a conical intersection (CI) mediated process as the one responsible for the formation of the cis isomer. The role of the hydrogen bond network of amino acids close to the chromophore in controlling the maximum absorption and the isomerization process has also been discussed, with particular emphasis on the function of Cys_{69}, Glu_{46}, and Tyr_{42}[6,11,12,14] residues. The possible electrostatic control exerted by the counterion of the chromophore (Arg_{52}) has also been addressed with conflicting results.[7,15] Moreover, a clear differentiation between the intrinsic properties of the chromophore and the effects of the protein in the full reaction process has remained elusive, in part due to the difficulties of performing experiments with anionic substances in vacuo, to the problems associated

* Corresponding author e-mail: pedro.brana@uv.es (P.B.C.), andres@qfa.uji.es (J.A.).

† Universidad de Valencia.

‡ Universidad de Oviedo.

§ Universidad Jaume I.

10.1021/ct900401z CCC: $40.75
Published on Web 09/24/2009

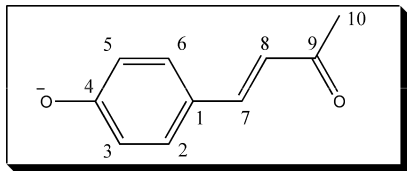

Figure 1. Model of the PYP chromophore considered in this study.

with the interpretation of the results obtained with the protein, and also to the complexities inherent in the theoretical modeling of large biological molecules and anionic systems, particularly when involved in excited state reactions. Thus, and despite all of the efforts carried out to date, this reaction remains not fully understood. Its complex nature, which combines short reaction times, different electronic states, and a complex anionic chromophore, turns this process into a challenge for both experimentalists and theoreticians. As a continuation of previous work[12] on the PYP photochemistry where the role of the protein in the control of the absorption wavelength was disentangled, we now focus on the intrinsic reactivity and structural properties of a model chromophore of the *p*-hydroxycinnamoyl anion (see Figure 1) in vacuo, as an initial step for understanding the possible role of the protein in the early events of the isomerization process. This model differs from the natural chromophore as well as other chromophore models used in previous works[3,4,8,10,11,16] dealing with different aspects of the photochemistry of PYP. The reason for selecting this model is twofold. On the one hand, the insights obtained with this reduced model, disentangled of the protein environment and linkage, will show the intrinsic behavior of the central structure and the isomerizing double bond[17] while at the same time allowing a differential comparison with the full protein. On the other hand, the results obtained can be compared with recent experimental observations where the fast dynamics of this chromophore were analyzed and proven to be similar (in the isomerization time and also in the coherence reflecting the involvement of low-frequency motions in isomerization[17]) to that of the protein. Furthermore, the nature of the lowest-lying electronic excited state is qualitatively similar (the dominant configuration is characterized by an excitation that involves the same kind of orbitals, and it also displays a significant value of the related oscillator strength) to that of the full protein model,[12] thus indicating that the model is a reliable one.

To tackle this problem, we employed a combined strategy based on the use of the minimum energy path (MEP) approach, which can be considered a zero-order static description of the reactive process that takes place in the first low-lying excited state (the bright $\pi \rightarrow \pi^*$ state, S_1), together with the application of the quantum theory of atoms in molecules (QTAIM)[18] for understanding the key changes in the molecular structure of the chromophore, an intrinsic aspect that may also help to shed light on the favorable reaction mechanism, while at the same time rendering some insight into the role of the protein. The theoretical description of reactive processes that take place in excited electronic states also needs a method that can describe in a balanced way all of the electronic states involved, which can be very different in their chemical nature.[19] The method must not only be qualitatively correct but also reasonably precise at a moderate computational cost. Moreover, it must also be able to describe situations where energetic degeneracy is present and nonadiabatic effects have a fundamental contribution. For molecules of this size, the CASPT2/CASSCF method (i.e., CASSCF optimizations followed by CASPT2 single-point computations) has proven to be a flexible as well as computationally affordable tool. It combines both the ability of describing in a balanced way electronic states of a different nature, which ultimately allows the method to characterize a full reaction path, with a reasonable accuracy, being able to account for the dynamic correlation effects. The reliability of this theoretical approach in the description of the kind of reactive process discussed here has been proven in similar[12] and related systems.[20−24]

Since rationalizing the chemical nature of excited electronic states is not always easy, we have used QTAIM[18] to avoid any methodological bias. This is a generalization of quantum mechanics to open systems that provides orbital invariant chemical bonding indicators and a topological partition of the physical space into quantum atoms which provide additive contributions to every global quantum mechanical expectation value (see Supporting Information for further details).

In this work, we will focus on the reaction path associated with the twisting of the C_7-C_8 double bond (see Figure 1) in the selected model chromophore. Even when it has been experimentally shown using blocked chromophores similar to the natural one that both single and double bond twisting can be active in the photochemical deactivation process, the C_7-C_8 double bond twisting has proven to be involved in the main reaction channel.[25] This has also been recently shown through direct observation of the fast in vacuo dynamics of the model chromophore used in this work.[17] Moreover, in the case of the chromophore embedded in the protein, single-bond twisting of the C_1-C_7 seems unlikely, as such a process will suffer the steric hindrance imposed by the protein structure. As a final result, we will also discuss the possible role that the triplet state can have in this and other photochemical processes carried out by biological photoreceptors.

2. Theoretical Methods

We have used the CASPT2/CASSCF strategy in the description of this photochemical process. The relevant critical points as well as the MEP optimized geometries in the S_1 potential energy surface (PES) have been located using a two-roots−equal-weights state average CASSCF level of theory (see Supporting Information for details). An active space that comprises 12 electrons in 11 π-like orbitals has been used. Due to the nature of the electronic states involved and its sensitivity to the quality of the basis set employed,[11] we have used a flexible and reasonably large ANO-S basis set[26] with contraction, C,O[4s3p1d]/H[2s1p]. To account for the dynamic correlation effects, at each optimized point we have carried out CASPT2 calculations using as reference wave functions those obtained at the six-roots−equal-weights state average CASSCF level with an active space of 16 electrons in 13 orbitals, where the *n* (lone pair) orbitals of both oxygen atoms were included, following the same strategy used in a previous work in the full (PYP) protein.[12]

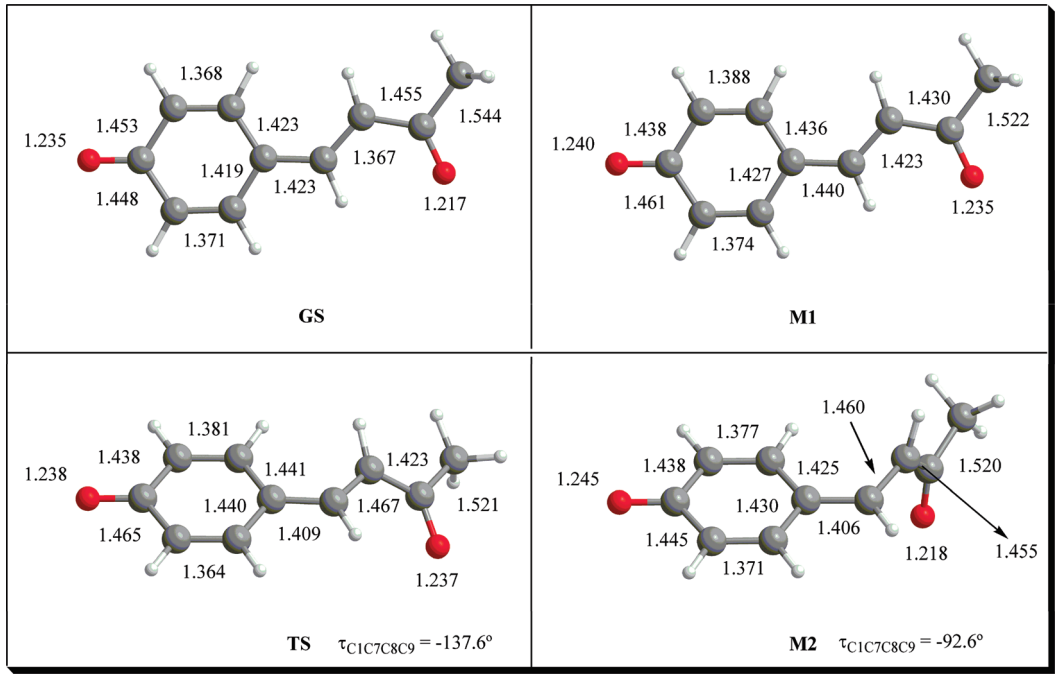

Figure 2. Most relevant geometrical parameters for the different equilibrium structures located in the S_0 and S_1 potential energy surfaces.

This protocol has also been employed to evaluate the position of the triplet and doublet (neutral) states. Throughout all of the CASPT2 computations, an imaginary level shift[27] of 0.2 au has been used to limit the effects of intruder states. All of the computations were carried out using the MOLCAS 7 program.[28] QTAIM analyses have been performed with the AIMPAC suite of programs[29] from the MOLCAS output wave functions. Care was taken that a full set of critical points (cp's) of the density was found at every stationary point, and bonding information was taken from standard scalars obtained at relevant (3,−1) cp's.

Some previous concerns about the applicability of the QTAIM to excited states[30] have now been fully rebutted,[31] and recent work[32] has shown that the theory may be used safely in these cases.

3. Results and Discussion

3.1. Geometries. In this subsection, we will describe the most relevant characteristics of the intermediates involved in the process. Figure 2 displays the optimized structures involved in the isomerization mechanism on both the S_0 and S_1 PES through the C_7-C_8 bond twisting, together with some selected geometrical parameters.

The corresponding values for both Mulliken population analysis (MPA) and Bader topological charges (BTC) are presented in Table 1. Although it is well-known that the former is both method- and basis-set-dependent, most computational chemists are used to their values. BTCs, on the other hand, are measurable quantum expectation values, routinely obtained from X-ray charge density crystallography[33] and much more stable versus changes in computational parameters. BTCs are usually larger than those of the MPA but reflect the actual distribution of electrons in real space, a particularly important point in excited states,

Table 1. Negative Charge Distribution (au) Computed Using Mulliken Population Analysis and Bader Topological Charges (between brackets) for All of the Equilibrium Structures Located along the Minimum Energy Path of the Model Chromophore[a]

	S_0		S_1	
structure	q_{ph}	q_{chain}	q_{ph}	q_{chain}
GS	−0.58 (−0.69)	−0.42 (−0.30)	−0.37 (−0.44)	−0.63 (−0.55)
M1	−0.55 (−0.67)	−0.45 (−0.32)	−0.38 (−0.47)	−0.62 (−0.53)
TS	−0.45 (−0.58)	−0.55 (−0.41)	−0.40 (−0.51)	−0.60 (−0.48)
M2	−0.10 (−0.26)	−0.90 (−0.73)	−0.64 (−0.75)	−0.36 (−0.24)

[a] q_{ph} stands for the charge located in the phenoxy ring, while q_{chain} is the charge located in the rest of the molecule.

where charge separations are much more likely to occur. Four stationary points, three minima (**GS**, **M1**, and **M2**) and a transition state (**TS**), have been characterized in the reaction path. **GS**, the trans ground state minimum structure, displays a geometry with some quinonic type character (see Figure 2), but just up to some degree; therefore, a clear characterization cannot be established. This behavior points to a delocalization of the negative charge throughout the structure, rather than to a concentration on the phenoxy moiety. Indeed, both MPA and BTC show the negative charge only partially localized on the phenoxy ring, with a significant amount of charge located in the carbon chain (see Table 1).

M1, the first minimum located in the S_1 reaction path, displays again a structure that seems to lose, at least partially, the quinonic-like character. This structure is characterized by a modification of the bond lengths of the carbon chain. In particular, an increase in the length of the (isomerizing) C_7-C_8 and C_1-C_7 bonds (yet, in the case of the last one, to a minor extent) is observed. The region of the keto group changes noticeably with respect to the **GS** structure, with an increase in the bond length of the C═O group and a decrease of the C_8-C_9 and C_9-C_{10} bond lengths. MPA and

Table 2. Relative Energies (to S_0, eV) and Oscillator Strengths (in parentheses) for the Most Significant Electronic States at the Franck−Condon Geometry Computed at the CASPT2/CASSCF/ANO-S Theoretical Level

electronic state	ΔE
S_1 ($\pi\rightarrow\pi^*$)	2.54 (0.928)
S_2 ($n\rightarrow\pi^*$)	3.48 ($<10^{-3}$)
S_3 ($\pi\rightarrow\pi^*$)	3.67 (0.092)
S_4 ($n\rightarrow\pi^*$)	3.72 ($<10^{-3}$)
D_1 ($\pi\rightarrow\pi^*$)	2.79
T_1 ($\pi\rightarrow\pi^*$)	1.83

BTC values are consistent with a situation where the negative charge is mainly localized at the carbon chain (see Table 1), with values very similar to those displayed by the bright (S_1) state at the Franck−Condon (FC) structure. **TS**, the transition state for the twisting of the C_7-C_8 bond in S_1, displays similar characteristics to those of the **M1** structure, except for the twisting of the C_7-C_8 bond and the increase of its length (see Figure 2). The C_1-C_7 bond also perceptibly shortens. MPA and BTC values show a negative charge distribution similar to the one found in **M1**. Finally, **M2**, the twisted minimum optimized in S_1, displays a nearly 90° twisted structure where the keto oxygen bond length has shortened and that of the C_8-C_9 bond has lengthened, rendering values similar to those found in the **GS** structure. MPA and BTC values indicate that part of the negative charge has moved from the carbon chain to the phenoxy ring when compared with the previous structures. As a result, it can be seen that both MPA and BTC render the same qualitative trend with a gradual partial localization of the negative charge in the phenoxy ring along the MEP.

3.2. Energies of the States and Minimum Energy Path. Table 2 shows the ordering of the lowest-lying electronic states at the FC point, whereas Figure 3 shows the MEP computed for the S_1 twisting process of the C_7-C_8 bond. The first thing to note is the energetic order of the different electronic states at the FC point. The lowest-lying

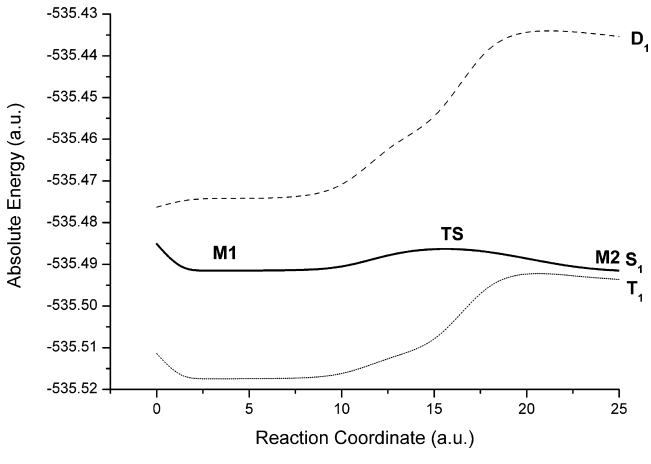

Figure 3. Graphical representation of the minimum energy path computed for the twisting of the C_7-C_8 bond in the lowest-lying singlet electronic state (S_1) at the CASPT2/CASSCF/ANO-S theoretical level (optimized structures along the path are indicated). The doublet (D_1) and triplet (T_1) states are also included.

singlet excited state of the anion is not metastable with respect to the autoionization process at the FC point.

As can be seen in Table 2, the neutral radical (D_1) is energetically less stable (2.79 eV vs 2.54 eV) than the S_1 $\pi\rightarrow\pi^*$ lowest-lying singlet state. This result is in line with the experimental results of Lee et al.,[17] where it is shown that the highest quantum yield is obtained for the reaction channel associated with the isomerization process. The results obtained are consistent with a process in which population of the neutral state would not be possible unless high excitation energies are used, with the system being excited either to a different electronic state (higher in energy than S_1, see Table 2) or to a high vibrational state; that is, the system becomes vibrationally hot in S_1. However, due to the relatively small energetic difference, we cannot rule out the possibility of regions of the potential energy surface close to the FC region where the anion becomes a metastable state. Special caution must be taken when analyzing those regions,[34,35] a problem that is out of the scope of this work and has previously been addressed using different computational methods.[10,11,16p]

Another point is that the computed S_0-S_1 vertical excitation energy is in line with previous results obtained for the full protein.[12] Despite both calculations cannot be directly compared due to the differences in the models and level of theory employed, this result is consistent with the proposal of Andersen and co-workers,[36] who suggested that the role of the protein is that of shielding the chromophore from the solvent (that would produce a large shift on the absorption maximum) and creating an environment similar to that of the chromophore in vacuo with a small difference in the absorption color due to the fine-tuning carried out by the protein. It must be stressed, however, that vertical excitation energy does not correspond in general to the absorption band maximum, yet a reasonable degree of agreement can be usually expected. More accurate comparisons would require calculation of the vibrational profile of the absorption band. It is also interesting to note that, for the carboxilate derivative of a related model of the PYP chromophore, the trans p-coumaric acid, some popular methods render significant and unexpected differences,[16q] pointing out that caution must be taken with the models and theoretical methods employed. Moreover, recent computational work has cast some doubt on the interpretation of photodestruction spectroscopy results in related systems.[37]

The following excited state, S_2, is of $n\rightarrow\pi^*$ type like S_4, whereas S_3 is again a $\pi\rightarrow\pi^*$ state. It is also interesting to note that both S_2 and S_4 show a clear multiconfigurational character, pointing out that only a method able to describe appropriately this characteristic can render a correct description of these states and their energies. In particular, the use of single-reference-based methods for the study of these kinds of states can be problematic. Moreover, the inclusion of dynamic correlation effects through CASPT2 single-point calculations alters the order and energy gap among the states (see Supporting Information), pointing out that the use of the CASSCF method for the computation of molecular dynamics must be carefully assessed.

Figure 3 shows a reaction profile in which, after an initial relaxation from the FC point and formation of the relaxed planar minimum **M1**, a small barrier (0.15 eV) must be surmounted to reach the twisted **M2** minimum, which is 0.19 eV more stable than the FC point, nearly degenerate with the lowest-lying triplet state (T_1), and 1.49 eV more stable than the neutral doublet state (D_1). Contrary to the behavior of D_1, T_1 is more stable than the lowest-lying singlet state (see also Table 2) along this reaction profile. As the reaction path proceeds, the energies of the S_1 and T_1 states approach and are almost degenerate in the region close to **M2**, the twisted minimum in S_1. Indeed, the differences in energy along the reaction path are virtually negligible soon after **TS** (see Figure 3). This fact may have important consequences for the reaction process, particularly under the experimental conditions used, characterized for the existence of an excess of energy. For the intersystem crossing (ISC)-mediated (S_1/T_1) process to be competitive with the internal conversion (CI)-mediated (S_1/S_0) one, this has to happen on a time scale on the same order as the one assigned for the S_1/S_0 nonradiative transition. The possible implications for the mechanism discussed here rely on the existence of such a competitive and fast ISC process operating simultaneously with the S_1/S_0 nonradiative relaxation. Lee et al.[17] give a time estimate for the latter of about 1 ps. This is not the usual time scale for an ISC process (with rough estimates[38] for an S_1/T_1 transition in the range 10^{-6} to 10^{-11} s) except for those systems where the spin−orbit coupling (SOC) is large (like transition metals). However, upon excitation to higher vibrational energies, the possibility of population of the T_1 state cannot be disregarded. It could be argued that the main interaction underlying the formation of the triplet state (T_1) after excitation to the first low-lying singlet excited state (S_1), the SOC, is not fast enough to compete with the nonradiative deactivation process mediated by a conical intersection. This may initially be thought to be due to the usually low values of the SOC obtained for polyenes, like the system studied here, when compared with other systems, where the SOC is a strong interaction that cannot be neglected in the study of reactive processes. Were this the case, the time needed for the transition from the S_1 to the T_1 state would be very long compared with the fast time scale proposed for the early events of the trans−cis isomerization reaction. However, when computing the rate constant for the ISC process using the Fermi golden rule approach (see eq 1), different factors contribute to the efficiency of ISC. One is, as already mentioned, the value of the SOC term.

$$k_{i\to f} = \frac{2\pi}{\hbar}\sum_{\{|f\rangle\}} |\langle i|\hat{H}'_{SO}|f\rangle|^2 \delta(E_i^0 - E_f^0) \quad (1)$$

The other one is the density of states, ρ_E. Thus, in order to determine the possible coexistence of a triplet deactivation channel, we have to analyze whether in the experimental conditions a high density of states is available (it is clear that the number of states that obey the resonance or near resonance condition will be larger provided that an excess of energy exists in the system, like the experimental conditions of Lee et al.[17]) and also determine the value of the SOC term. It is in the evaluation of this term that some care must be taken. As has been recently shown,[39] the vibronic contribution to the SOC (see eq 2) can produce an important effect (of several orders of magnitude in molecules of moderate size[39]) in the nonradiative relaxation mediated by a S/T crossing. Both aspects, the density of states available at the experimental conditions and the SOC value including the first-order vibrational term,

$$\langle i, v|\hat{H}'_{SO}|f, v'\rangle = \langle i|\hat{H}'_{SO}|f\rangle|_{q_0=0}\langle v|v'\rangle + \sum_k \left(\frac{\partial}{\partial_{q_k}}\langle i|\hat{H}'_{SO}|f\rangle\right)_{q_0=0}\langle v|q_k|v'\rangle + O(|q|^2) \quad (2)$$

will contribute to increase the value of $k_{i\to f}$ giving rise to a fast intersystem crossing process. It is interesting to note that, when the energetic levels lie close in energy, the overlap between the vibrational wave functions will be non-negligible, with an important contribution of the Franck−Condon factors. Moreover, in the region of the MEP where a near energetic degeneracy between S_1 and T_1 exists, the molecule is twisted, and therefore, the out-of-plane deformations will increase the SOC coupling between $\pi \rightarrow \pi^*$ states through the second term in eq 2. This competitive process could be even more important inside the protein, where a high ρ_E exists in the region of ISC. Experimental monitoring of the formation of a putative triplet species[40] would be highly desirable to test the validity and generality of this proposal, particularly in the protein environment. However, it has to be stressed that population of the triplet state would be a process leading to a decrease in the efficiency of the protein to carry out its sensory role, so the impact of this putative competitive deactivation channel in the natural photochemical reaction has to be minimized in favor of the trans-to-cis isomerization one. This can be accomplished by turning the region around **M2** into a conical intersection seam, as proposed in ref 6.

3.3. QTAIM Analysis of the Excited States. Table 3 contains the most significant structural indicators for the isomerizing double bond at all of the significant equilibrium

Table 3. Relevant Structural Information [Eigenvalues of the Hessian of the Density (λ_1, λ_2, λ_3), Ellipticity (ε), Value of the Density at the Critical Point (ρ_c), and Value of the Laplacian of the Density at the Critical Point ($\nabla^2\rho_c$)] Obtained Using QTAIM for the Isomerizing Double Bond in All of the Equilibrium Structures Located along the Reaction Path

structure	λ_1[a]	λ_2[a]	λ_3[a]	ε	ρ_c[a]	$\nabla^2\rho_c$[a]
GS	-7.51×10^{-1}	-5.97×10^{-1}	2.01×10^{-1}	2.57×10^{-1}	3.34×10^{-1}	-1.15×10^{0}
M1	-6.45×10^{-1}	-5.40×10^{-1}	2.60×10^{-1}	1.96×10^{-1}	2.99×10^{-1}	-9.24×10^{-1}
TS	-5.65×10^{-1}	-5.18×10^{-1}	2.93×10^{-1}	9.10×10^{-2}	2.75×10^{-1}	-7.91×10^{-1}
M2	-5.58×10^{-1}	-5.28×10^{-1}	2.84×10^{-1}	5.62×10^{-2}	2.78×10^{-1}	-8.03×10^{-1}

[a] Values are given in au.

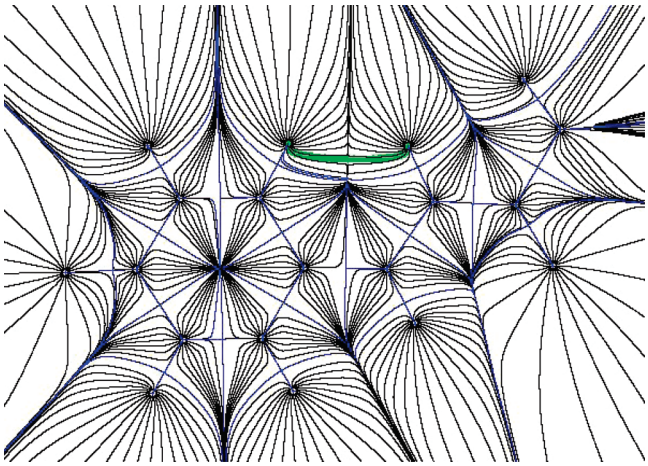

Figure 4. Plot of the gradient field lines of the electronic density (ρ) for the **M1** intermediate. The green line is the bond path of the H−H bonding interaction.

structures located for this process obtained with the QTAIM method (see the Supporting Information for a brief description of their meaning). As shown in Table 3, the decrease in the values of the ellipticity (ε) and the density (ρ_c) at the bond critical point as well as the negative values of the laplacian of the density ($\nabla^2\rho_c$) at the bond critical point are consistent with a mechanism in which the covalent C_7-C_8 bond modifies its character from double-like to single-like (see Supporting Information). The weakening of the isomerizing double bond in S_1 is expected to facilitate the trans-to-cis transformation.

A remarkable result is the appearance of a new ring critical point in **M1** as a consequence of the formation of a H−H bond. Accordingly, **M1** displays the bonding pattern depicted in Figure 4. The energetic stabilization created by the formation of this bonding interaction in this planar structure is estimated to be about 3−4 kcal/mol,[41] which is on the same order or magnitude of the energy stabilization of this minimum compared to **TS** and seems to indicate that it is associated with the existence of a small barrier for the process in vacuo. It is interesting to note that such a kind of planar structure is not found in the S_1 state of the protein as a consequence of the steric restrictions existing in the protein binding pocket, which forces the chromophore to adopt a slightly bandy structure.[12] This distortion from planarity in the protein environment will induce a chromophore structure where the hydrogen atoms involved in the H−H bond will move further away. As a result, it is expected that the stabilization generated through this bonding interaction will at least decrease or even disappear, and the S_1 minimum in the protein (equivalent to **M1**) can then become a shallow one. This may ultimately lead to a faster process due to the decrease (or even disappearance) of the barrier in the lowest-lying excited state. Such a kind of profile is also present in other proteins that perform a similar role.[23] Thus, the PYP protein not only would act as a shield avoiding the interaction of the solvent with the chromophore,[36] but it could also modulate the S_1 profile, improving the efficiency of the mechanism when the process takes place with a moderate excess of energy, which should be the case under natural conditions.

4. Conclusions

We have analyzed the excited state isomerization process of a model of the PYP chromophore in vacuo combining the energetic analysis based on the MEP approach with the QTAIM theory at the CASPT2/CASSCF multiconfigurational level. We have shown that the isomerization process through direct twisting of the C_7-C_8 double bond leads to a reaction profile with a small barrier in the excited state. This barrier could in part be originated by the formation of a prereactive planar intermediate characterized by the existence of a bonding H−H interaction that contributes to enhancing its energetic stability. This behavior is not expected to be present at the same extent in the PYP where the steric interactions existing in the protein binding pocket will prevent the chromophore of adopting a planar structure, pointing to one possible role of the protein in modulating the efficiency of this reaction. We have also analyzed the role of the triplet state in the general reactive process. The possibility of competition between the population of the triplet state and the trans/cis isomerization process has been critically discussed, and new experimental studies are suggested. A possible role of the PYP protein in the enhancement of the isomerization process efficiency has also been proposed. We hope the results outlined will be helpful not only for a better understanding of the photochemistry of PYP but also for a general understanding of photochemical processes in biological photoreceptors.

Acknowledgment. Financial support is acknowledged from MEC/MICINN/FEDER projects CTQ2007-61260 and CSD2007-0010 Consolider-Ingenio in Molecular Nanoscience, contract Juan de la Cierva (PBC), and FPU grant (DRS), from Generalitat Valenciana, project GVPRE/2008/059, and from Universitat de València, project UV-EQUIP09-5764. The authors wish to thank Prof. M. Merchán and Prof. M. Olivucci for helpful discussions.

Note Added after ASAP Publication. This article was released ASAP on September 24, 2009 with minor errors in the Results and Discussion section. The correct version was posted on September 29, 2009.

Supporting Information Available: Further details of the theoretical methods used, geometries, absolute energies, and MPA and BTA charges for all of the stationary structures located. This information is available free of charge via the Internet at http://pubs.acs.org/.

References

(1) Hellingwerf, K. J.; Hendriks, J.; Gensch, T. *J. Phys. Chem. A* **2003**, *107*, 1082, and references therein.

(2) Cusanovich, M. A.; Meyer, T. E. *Biochemistry* **2003**, *42*, 4759, and references therein.

(3) Molina, V.; Merchán, M. *Proc. Natl. Acad. Sci. U. S. A.* **2001**, *98*, 4299–4304.

(4) Thompson, M. J.; Bashford, D.; Noodleman, L.; Getzoff, E. D. *J. Am. Chem. Soc.* **2003**, *125*, 8186–8194.

(5) Yamada, A.; Ishikura, T.; Yamato, T. *Proteins* **2004**, *55*, 1063–1069.

(6) Groenhof, G.; Bouxin-Cademartory, M.; Hess, B.; de Visser, S. P.; Berendsen, H. J. C.; Olivucci, M.; Mark, A. E.; Robb, M. A. *J. Am. Chem. Soc.* **2004**, *128*, 4228–4233.

(7) Groenhof, G.; Schäfer, L. V.; Boggio-Pasqua, M.; Grubmüller, H.; Robb, M. A. *J. Am. Chem. Soc.* **2008**, *130*, 3250–3251.

(8) Heyne, K.; Mohammed, O. F.; Usman, A.; Dreyer, J.; Nibbering, E. T. J.; Cusanovich, M. A. *J. Am. Chem. Soc.* **2005**, *127*, 18100–18106.

(9) Matsuura, A.; Sato, H.; Houjou, H.; Saito, S.; Hayashi, T.; Sakurai, M. *J. Comput. Chem.* **2006**, *27*, 1623–1630.

(10) Gromov, E. V.; Burghardt, I.; Köppel, H.; Cederbaum, L. S. *J. Am. Chem. Soc.* **2007**, *129*, 6798–6806.

(11) Gromov, E. V.; Burghardt, I.; Hynes, J. T.; Köppel, H.; Cederbaum, L. S. *J. Photochem. Photobiol. A* **2007**, *190*, 241–257.

(12) Coto, P. B.; Martí, S.; Oliva, M.; Olivucci, M.; Merchán, M.; Andrés, J. *J. Phys. Chem. B* **2008**, *112*, 7153–7156.

(13) Ko, C.; Virshup, A. M.; Martínez, T. J. *Chem. Phys. Lett.* **2008**, *460*, 272–277.

(14) van Wilderen, L. J. G. W.; van der Horst, M. A.; van Stokkum, I. H. M.; Hellingwerf, K. J.; van Grondelle, R.; Groot, M. L. *Proc. Natl. Acad. Sci. U. S. A.* **2006**, *103*, 15050–15055.

(15) Changenet-Barret, P.; Plaza, P.; Martin, M. M.; Chosrowjan, H.; Taniguchi, S.; Mataga, N.; Imamoto, Y.; Kataoka, M. *Chem. Phys. Lett.* **2007**, *434*, 320–325.

(16) See, among others: (a) He, Z.; Martin, C. H.; Birge, R.; Freed, K. F. *J. Phys. Chem. A* **2000**, *104*, 2939–2952. (b) Sergi, A.; Grüning, M.; Ferrario, M.; Buda, F. *J. Phys. Chem. B* **2001**, *105*, 4386–4391. (c) Yoda, M.; Houjou, H.; Inoue, Y.; Sakurai, M. *J. Phys. Chem. B* **2001**, *105*, 9887–9895. (d) Yamada, A.; Yamamoto, S.; Yamato, T.; Kakitani, T. *THEOCHEM* **2001**, *536*, 195–201. (e) Unno, M.; Kumauchi, M.; Sasaki, J.; Tokunaga, F.; Yamauchi, S. *Biochemistry* **2002**, *41*, 5668–5674. (f) Ko, C.; Levine, B.; Toniolo, A.; Manohar, L.; Olsen, S.; Werner, H.-J.; Martínez, T. J. *J. Am. Chem. Soc.* **2003**, *125*, 12710–12711. (g) Toniolo, A.; Granucci, G.; Martínez, T. J. *J. Phys. Chem. A* **2003**, *107*, 3822–3830. (h) Unno, M.; Kumauchi, M.; Sasaki, J.; Tokunaga, F.; Yamauchi, S. *J. Phys. Chem. B* **2003**, *107*, 2837–2845. (i) Chosrowjan, H.; Taniguchi, S.; Mataga, N.; Unno, M.; Yamauchi, S.; Hamada, N.; Kumauchi, M.; Tokunaga, F. *J. Phys. Chem. B* **2004**, *108*, 2686–2698. (j) Premvardhan, L. L.; Buda, F.; van der Horst, M. A.; Lührs, D. C.; Hellingwerf, K. J.; van Grondelle, R. *J. Phys. Chem. B* **2004**, *108*, 5138–5148. (k) El-Mashtoly, S. F.; Unno, M.; Kumauchi, M.; Hamada, N.; Fujiwara, K.; Sasaki, J.; Imamoto, Y.; Kataoka, M.; Tokunaga, F.; Yamauchi, S. *Biochemistry* **2004**, *43*, 2279–2287. (l) Li, Q.-S.; Fang, W.-H. *Chem. Phys.* **2005**, *313*, 71–75. (m) Gromov, E. V.; Burghardt, I.; Köppel, H.; Cederbaum, L. S. *J. Phys. Chem. A* **2005**, *109*, 4623–4631. (n) de Groot, M.; Buma, W. J.; Gromov, E. V.; Burghardt, I.; Köppel, H.; Cederbaum, L. S. *J. Chem. Phys.* **2006**, *125*, 204303(17). (o) Unno, M.; Kumauchi, M.; Tokunaga, F.; Yamauchi, S. *J. Phys. Chem. B* **2007**, *111*, 2719–2726. (p) Muguruza González, E.; Guidoni, L.; Molteni, C. *Phys. Chem. Chem. Phys.* **2009**, *11*, 4556–4563. (q) Rocha-Rinza, T.; Christiansen, O.; Rajput, J.; Gopalan, A.; Rahbek, D. B.; Andersen, L. H.; Bochenkova, A. V.; Granovsky, A. A.; Bravaya, K. B.; Nemukhin, A. V.; Christiansen, K. L.; Brøndsted Nielsen, M. *J. Phys. Chem. A* **2009**, *113*, 9442–9449.

(17) Lee, I.-R.; Lee, W.; Zewail, A. H. *Proc. Natl. Acad. Sci. U. S. A.* **2006**, *103*, 258–262.

(18) Bader, R. F. W. *Atoms in Molecules: A Quantum Theory*; Oxford University Press: New York, 1994; pp 1−438.

(19) Roos, B. O.; Fülscher, M. P.; Malmqvist, P.-Å; Serrano-Andrés, L.; Pierloot, K.; Merchán, M. *Adv. Chem. Phys.* **1996**, *93*, 219–331.

(20) Coto, P. B.; Strambi, A.; Ferré, N.; Olivucci, M. *Proc. Natl. Acad. Sci. U. S. A.* **2006**, *103*, 17154–17159.

(21) Coto, P. B.; Sinicropi, A.; De Vico, L.; Ferré, N.; Olivucci, M. *Mol. Phys.* **2006**, *104*, 983–991.

(22) Strambi, A.; Coto, P. B.; Ferré, N.; Olivucci, M. *Theor. Chem. Acc.* **2007**, *118*, 185–191.

(23) Strambi, A.; Coto, P. B.; Frutos, L. M.; Ferré, N.; Olivucci, M. *J. Am. Chem. Soc.* **2008**, *130*, 3382–3388.

(24) Coto, P. B.; Strambi, A.; Olivucci, M. *Chem. Phys.* **2008**, *347*, 483–491.

(25) El-Gezawy, H.; Rettig, W.; Danel, A.; Jonusauskas, G. *J. Phys. Chem. B* **2005**, *109*, 18699–18705.

(26) Pierloot, K.; Dumez, B.; Widmark, P. O.; Roos, B. O. *Theor. Chim. Acta* **1995**, *90*, 87–114.

(27) Forsberg, N.; Malmqvist, P.-Å. *Chem. Phys. Lett.* **1997**, *274*, 196–204.

(28) Karlström, G.; Lindh, R.; Malmqvist, P.-Å.; Roos, B. O.; Ryde, U.; Veryazov, V.; Widmark, P.-O.; Cossi, M.; Schimmelpfennig, B.; Neograd y, P.; Seijo, L. *Comput. Mater. Sci.* **2003**, *28*, 222–239.

(29) Biegler-König, F. W.; Bader, R. F. W.; Ting-Hua, T. *J. Comput. Chem.* **1982**, *3*, 317–328.

(30) Cassam-Chenaï, P.; Jayatilaka, D. *Theor. Chem. Acc.* **2001**, *105*, 213–218.

(31) Popelier, P. L. A. *Struct. Bonding (Berlin)* **2005**, *115*, 1–56.

(32) Wang, Y.-G.; Wiberg, K. B.; Werstiuck, N. H. *J. Phys. Chem. A* **2007**, *111*, 3592–3601.

(33) Bader, R. F. W.; Matta, C. F. *J. Phys. Chem. A* **2004**, *108*, 8385–8394.

(34) Sommerfeld, T.; Riss, U. V.; Meyer, H.-D.; Cederbaum, L. S.; Engels, B.; Suter, H. U. *J. Phys. B: At., Mol. Opt. Phys.* **1998**, *31*, 4107–4122.

(35) Epifanovski, E.; Polyakov, I.; Grigorenko, B.; Nemukhin, A.; Krylov, A. I. *J. Chem. Theor. Comput.* **2009**, *5*, 1895–1906.

(36) Nielsen, I. B.; Boyé-Péronne, S.; El Ghazaly, M. O. A.; Kristensen, M. B.; Brøndsted Nielsen, S.; Andersen, L. H. *Biophys. J.* **2005**, *89*, 2597–2604.

(37) Filippi, C.; Zaccheddu, M.; Buda, F. *J. Chem. Theory Comput.* **2009**, *5*, 2074–2087.

(38) Klessinger, M.; Michl, J. *Excited States and Photochemistry of Organic Molecules*; VCH Publishers Inc.: New York, 1995; p 247.

(39) Tatchen, J.; Gilka, N.; Marian, C. M. *Phys. Chem. Chem. Phys.* **2007**, *9*, 5029–5221.

(40) It is interesting to note that data of ref 17 show the existence of a long-lived (58 ps) intermediate that could match with triplet state population.

(41) Martín-Pendás, A.; Francisco, E.; Blanco, M. A.; Gatti, C. *Chem.—Eur. J.* **2007**, *13*, 9362–9371.

CT900401Z